



Natural and artificial gamma-emitting radionuclides in volcanic soils of the Western Canary Islands

María López-Pérez^a, Candelaria Martín-Luis^b, Francisco Hernández^a, Esperanza Liger^c, José Carlos Fernández-Aldecoa^a, José Miguel Lorenzo-Salazar^a, José Hernández-Armas^a, Pedro A. Salazar-Carballo^{a,d,*}

^a Laboratorio de Física Médica y Radioactividad Ambiental, SEGAI, Universidad de La Laguna, Spain

^b Departamento Biología Animal, Edafología y Geología, Universidad de La Laguna, Spain

^c Departamento de Física Aplicada II, Universidad de Málaga, Spain

^d Departamento de Medicina Física y Farmacología, Universidad de La Laguna, Spain

ARTICLE INFO

Keywords:

Environmental radioactivity
Outdoor gamma radiation
Absorbed dose
¹³⁷Cs
Volcanic soils
Canary Islands

ABSTRACT

Terrestrial gamma absorbed dose rates as well as spatial distribution of gamma-emitting radionuclides ⁴⁰K, ²²⁶Ra and ²³²Th and ¹³⁷Cs in soils, are provided in detail for the first time in the Western Canary Islands.

The distribution of terrestrial gamma absorbed dose rates and the activity concentrations of ⁴⁰K, ²²⁶Ra and ²³²Th are discussed with respect to the main lithologies and geological features of each island. The average terrestrial absorbed dose rate (71.4 nGy·h⁻¹) reported here was slightly higher to previously reported values for the Eastern islands of this archipelago (43 nGy·h⁻¹) and close to the world's average (59 nGy·h⁻¹).

Relatively high ¹³⁷Cs activity concentrations, up to 100 Bq·kg⁻¹, were measured in some of the collected samples. To understand the origin of these activities, we compared the results from two different field surveys performed in 1991 and in 2013. The activity concentrations were found to be rather similar despite the 22 years gap between the measurements. Complementary radiometric data from aerosol samples collected at this site show that there are additional contributions of ¹³⁷Cs to this site produced by the deposition of dust particles brought by Saharan dust storms.

In terms of radiological risk, the gamma absorbed doses reported (external exposure) pose no risk to the local population. However, the contribution of the soil ¹³⁷Cs activity concentrations to the gamma absorbed dose were as high as 50% in some few locations.

1. Introduction

The determination of natural and artificial radionuclides is important from the radiation protection point of view. However, radionuclides can also be used as tracers of environmental processes in the ground, water, atmosphere, soil erosion, sedimentation and geochronology, marine ecosystems studies, studies related to climate change and aerosols and transportation of air masses studies (Anagnostakis, 2015; Carroll and Lerche, 2010; Cartwright et al., 2017; Hirayama et al., 2020). Understanding the distribution of radionuclides in soils is essential to many of these environmental studies because soils act as a channel for transferring radionuclides to plants, animals and to other environmental compartments, such as water and air (Navas et al., 2007; Seaman and Roberts, 2012).

Natural terrestrial gamma radiation originates from the upper layers of soil, and depends on its radio-geochemical composition, mainly ²²⁶Ra (²³⁸U), ²³²Th, and ⁴⁰K. These radionuclides are generally not homogeneously distributed in soils. Their concentration depends on geological factors and to a lesser extent upon biological, atmospheric and anthropogenic interactions. Studying the spatial distribution of such radioisotopes and the associated emitted gamma radiation is important to assess the health risk to the general population (Filgueiras et al., 2020; Maxwell et al., 2020; Shahrokhi et al., 2021).

Man-made ¹³⁷Cesium (half-life 30.2 years) originates from a variety of sources. Large amounts of this artificial radionuclide were released into the environment due to global nuclear weapon testing carried out from the 1950s to the 1970s (referred to as bomb-derived or fallout ¹³⁷Cs) and by nuclear power plant accidents, among which, the most

* Corresponding author at: Laboratorio de Física Médica y Radioactividad Ambiental, SEGAI, Universidad de La Laguna, Spain.

E-mail address: psalazar@ull.edu.es (P.A. Salazar-Carballo).

<https://doi.org/10.1016/j.gexplo.2021.106840>

Received 14 December 2020; Received in revised form 4 June 2021; Accepted 10 June 2021

Available online 16 June 2021

0375-6742/© 2021 Elsevier B.V. All rights reserved.

important were the Chernobyl accident in 1986 and the Fukushima Daiichi accident in 2011 (the term Chernobyl or Fukushima ^{137}Cs is used). Understanding the magnitude of the fallout of this radionuclide is crucial not only to establish a baseline in case of future inputs but also to define a baseline for geomorphological reconstructions of soil redistribution due to erosion processes (Meusburger et al., 2020). Moreover, observations from terrestrial environments, which hosts radionuclides for many years after initial deposition, are key for health and environmental assessments (Evangelidou et al., 2016). Although ^{137}Cs occurs, in most sites, as a product of direct atmospheric fallout (Baggoura et al., 1998; Itthipoonthanakorn et al., 2019; McKenzie and Dulai, 2017), it can also be transported attached to dust particles, e.g. Saharan dust storms (Hernandez et al., 2007; Karlsson et al., 2008; López-Pérez et al., 2020) and smoke particles, e.g. forest fires from contaminated locations (Wotawa et al., 2006). Fukushima ^{137}Cs was measured in aerosol filters collected in the Canary Islands despite the large distance to the source (López-Pérez et al., 2013).

Studies related to the determination of natural gamma radiation have been published for the Eastern Canary Islands (Arnedo et al., 2017), and the island of Tenerife (Fernández-Aldecoa et al., 1992). In addition, a general study of ^{238}U , ^{232}Th and ^{40}K content in main lithotypes of the Canary Islands was published by (Hernández-Gutiérrez et al., 2011). However, the spatial distribution of ^{137}Cs in soils has not been reported before for this region.

The objectives of this work were: (1) to determine the concentration activities and spatial distribution of the terrestrial gamma absorbed doses at 1 m above the ground; (2) to establish the spatial distribution of ^{40}K , ^{226}Ra and ^{232}Th and ^{137}Cs concentration activities in the soils; (3) to assess the influence of the geological setting into the distribution of the terrestrial absorbed doses and natural gamma-emitting radionuclides; and (4) to assess the relatively high concentrations (80–100 $\text{Bq}\cdot\text{kg}^{-1}$) of ^{137}Cs measured in some of the soil samples collected at the study area.

To this purpose, we provide herein maps of the outdoor gamma absorbed dose rate measured in a field survey carried out in 2013 in the Western Canary Islands (including Tenerife, La Palma, La Gomera and El Hierro). We also provide maps of the natural gamma emitters (^{40}K , ^{226}Ra and ^{232}Th) and of ^{137}Cs in soil samples collected in the same field survey in 2013. In addition, geological maps showing the main lithological features of the islands are also provided for comparison purposes.

To put into perspective, the ^{137}Cs concentrations determined in the field survey in 2013, an unpublished dataset of ^{137}Cs concentrations in soil samples from an earlier field survey performed in 1991 (22 years before), overlapping the same studied areas, is reported herein. The comparison of both ^{137}Cs data sets provides a unique opportunity to obtain retrospective information on this artificial radionuclide in the

soils of these volcanic islands.

2. The study area

The Canary Islands, Fig. 1, located northwest of the African coast, are an active volcano archipelago, where all islands, except La Gomera, present signs of Holocene volcanism (Troll and Carracedo, 2016).

The Canary Islands have had a long eruptive history, ranging from at least 20 Ma (millions of years) in the eastern Canaries to ca. less than 1 to 4 Ma on the westernmost ones. Their geological evolution comprises at least three growth stages represented by three main units: 1) basal complexes (submarine or seamount stage), composed of turbiditic sediments and submarine volcanic rocks intruded by dike swarms and by plutonic bodies; 2) shield volcano edifices (initial subaerial stage or shield stage); and 3) post-shield cones and associated lava flows (Carracedo et al., 2002). These successive stages are commonly separated by erosive gaps, sometimes lasting several million years. In addition, giant landslides have occurred in all the islands (Coello-Bravo et al., 2020; Ferrer et al., 2013; Hunt et al., 2014). Recent and historical volcanism has also shaped the top most layer of the soil surface, mostly in Tenerife, La Palma and El Hierro islands, where lava flows and pyroclastic deposits cover a significant part of the island surfaces (Troll and Carracedo, 2016).

3. Materials and methods

3.1. Sampling strategy and soil sample preparation

To obtain a representative dose map of the gamma radiation in the Western Canary Islands, a regular sampling grid (3 × 3 km) was designed to determine the number of measurements necessary to be carried out on each island. The sampling survey was performed during the dry months (summer/autumn) of 2013. The number of sampling sites were: 226 (Tenerife), 79 (La Palma), La Gomera (40) and 30 (El Hierro) (see Fig. SM1). Before performing the fieldwork, each grid was visualized using digital cartography based on Google Earth to search for adequate sampling sites. Each sampling site was selected according to parameters such as accessibility, flatland surfaces and minimum distance from nearby building constructions and road surfaces, ca. 50 and 15 m, respectively. Due to the topographic characteristics of each island, some sampling sites were newly adjusted in situ before empirical measurements were taken.

In order to obtain the spatial distribution of ^{40}K , ^{226}Ra , ^{232}Th and ^{137}Cs soil activity concentrations in the studied areas, 121 soil samples were collected in a subset of the locations. Tenerife resulted in the most

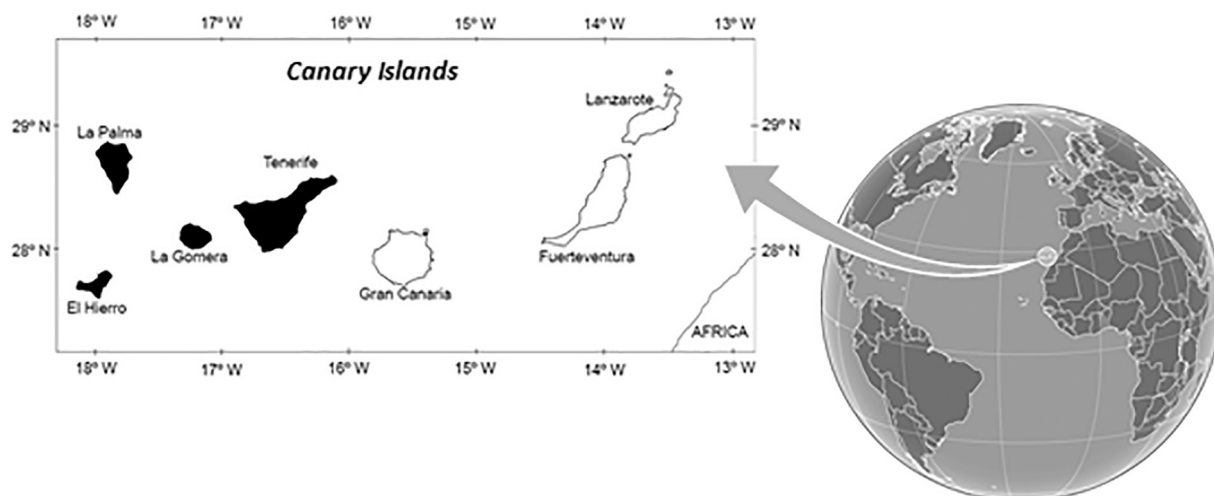


Fig. 1. Geographic location of the Canary Islands. In black, the islands studied in this work.

sampled island with 73 samples, La Palma with 25, and La Gomera and El Hierro with 13 and 10 soil samples, respectively (see Fig. 1 and Fig. SM1). Soil samples were collected at a depth of approximately 0–15 cm from uncultivated fields using a sampling area of 2 m². Before sampling, the ground surface was cleared of vegetation, roots and stones, and 1 kg of soil sample was taken using sampling metallic tubes according to (Herranz et al., 2003; UNE, 2002a). Then, soil samples were sealed and stored in plastic containers. Once in the laboratory, soil samples were dried at room temperature for 24 h and afterward at 105 °C until constant weight. The samples were pulverized, homogenized, and sieved using a 0.5 mm mesh (Baeza et al., 2003; UNE, 2002b). The sieved soil samples were weighed and transferred to a Marinelli beaker (500 ml capacity), carefully sealed, and stored for four weeks to allow for secular equilibrium between thorium, radium and their decay products.

3.2. Outdoor gamma absorbed dose rate measurements

A portable environmental gamma radiation meter MINI 6–80 (Mini-Instruments) equipped with an energy compensated detector (Geiger-Müller tube, MC-71) with low intrinsic background was used to determine the total absorbed dose rate. The detector was conveniently calibrated by the “Centro de Investigaciones Energéticas, Medioambientales y Tecnológicas (CIEMAT)”, Madrid, Spain.

The inherent detector background was determined from measurements taken in a plastic boat at sea level, approximately 2 km from the shore where the water depth was 150 m. The cosmic radiation value at sea level was computed from Eq. (1) and the background contribution was obtained as the difference between the experimental gamma absorbed dose rate and the cosmic radiation value.

$$E(z) = E(0) [a e^{-\alpha z} + b e^{\beta z}] \quad (1)$$

where $E(z)$ is the absorbed dose rate due to cosmic background at z kilometres of altitude; $E(0)$ is the reference value measured at sea level, and equal to 30 nGy·h⁻¹ at the latitude of Canary Islands (value obtained using PARMA software (Sato, 2015); and $a = 0.21$; $\alpha = 1.6 \text{ km}^{-1}$; $b = 0.80$ and $\beta = 0.45 \text{ km}^{-1}$).

Outdoor gamma radiation measurements were obtained by placing the detector 1 m above the ground. Altitude, GPS geo-localization and environmental data such as temperature, pressure and humidity were also collected. GPS coordinates were converted to standard UTM coordinates. Five different 1-min measurements were obtained at each site and the average value was calculated.

To estimate the terrestrial gamma absorbed dose – i.e., the dose due to radiation from gamma-emitting radionuclides present in the soil – at each sampling site, the cosmic radiation contribution was subtracted from the experimental values. To this end, the cosmogenic contribution was calculated, according to (UNSCEAR, 1993), using Eq. (1).

Contour maps of outdoor gamma absorbed dose rate and for the ⁴⁰K, ²²⁶Ra, ²³²Th and ¹³⁷Cs activity concentration for each island were built by ordinary kriging interpolation. Such probabilistic interpolation methodology is based on the spatial arrangement of the empirical observations and allows to obtain the distribution of the experimental variable in the whole studied area. This method is based on the spatial correlation of the data (semivariogram). For details see (Caro et al., 2013).

3.3. Gamma spectrometry of soil samples

All the radiometric measurements were performed by low-level high-resolution gamma spectrometry with coaxial-type germanium detectors (Canberra Industries Inc., USA). These detectors are enclosed in 15 cm old iron-shields inside a clean laboratory. The laboratory is kept under positive pressure to minimize the concentration of radon in the indoor air. These detectors are calibrated using certified reference gamma-ray

cocktails purchased from the National Physical Laboratory (United Kingdom). The laboratory measurements are subjected to a regular quality control program including periodical monitoring of the backgrounds, calibrations, and the detection system performances.

The activity concentration of ²²⁶Ra, ²³²Th, ⁴⁰K and ¹³⁷Cs in soil samples were measured throughout 1 to 3 days, and 7 days for background measurements. Gamma spectra analyses, including background correction, were performed with the Genie2K spectrometry software version 2.0 (Canberra Industries Inc., USA).

The activity concentration of ²²⁶Ra was obtained from the ²¹⁴Pb gamma-ray line of 351.92 keV (ca. 37.20% intensity). The ²³²Th activity concentration was determined from both ²²⁸Ac and ²⁰⁸Tl gamma-ray lines of 911.60 keV (ca. 27.70% intensity) and 583.19 keV (ca. 84.50% intensity), respectively. Finally, the activity concentrations of ⁴⁰K and ¹³⁷Cs were directly measured by their gamma-ray peaks at 1460.81 keV (ca. 10.67% intensity) and 661.65 KeV (ca. 85.12% intensity), respectively. The Minimum Detectable Activity (MDA) for each studied radionuclide was 0.29 (²¹⁴Pb), 0.40 (²²⁸Ac), 0.10 (²⁰⁸Tl), 1.59 (⁴⁰K) and 0.08 (¹³⁷Cs) Bq·kg⁻¹.

To validate the measurement methods, our laboratory routinely participates in interlaboratory comparisons of gamma-emitting radionuclides in soils, organized by the International Atomic Energy Agency (IAEA) and the Spanish Nuclear Safety Council (CSN). The z-score test in the most recent intercomparison (2019) was below 2 for all the tested radioactivity parameters, which assure the accuracy and repeatability of our processes and measurements.

The method used to determine ¹³⁷Cs activity concentrations in the soil samples collected in 1991 was exactly the same as reported above, though the sampling strategy was slightly different as it was performed as part of an earlier research project carried out in these western islands (Fernández de Aldecoa, 2000). Top-soil samples ($n = 131$) were collected, prepared and measured by gamma spectrometry. Sampling sites were arranged in a similar grid over the area in each of the four islands, with 103, 12, 10 and 6 sampling sites for Tenerife, La Palma, La Gomera and El Hierro, respectively (see Fig. 1).

4. Results and discussion

4.1. Outdoor gamma absorbed dose rate in air

The 2013 survey of gamma absorbed dose measurements covered about 95% of the whole studied territory. In Tenerife (TF) the coverage reached a value of 91% of the planned sampling grid, with the exception of the northern flank of Teide volcano due to accessibility restrictions. Similarly, a coverage level of 90% was reached in La Palma (LP). In La Gomera (GO) and El Hierro (HI) the coverage level was 100%.

The geometric mean and the geometric standard deviation (GSD)

Table 1

Geometric mean (GM) and geometric standard deviation (GSD) of the total gamma absorbed dose rate, and for the cosmic and terrestrial contributions, averaged in the Western Canary Islands.

Island	Number of measurements	Total absorbed dose rate (nGy/h)		Cosmic contribution (nGy/h)		Terrestrial contribution (nGy/h)	
		G. mean	GSD	G. mean	GSD	G. mean	GSD
TF	206	144	1.3	37.4	1.3	94.6	1.4
LP	71	103	1.6	36.5	1.2	44.7	1.5
GO	41	82.7	1.2	35.8	1.1	37.2	1.2
HI	34	112	1.1	34.5	1.1	67.1	1.2
Western Canary Islands	352	126.7	1.3	36.6	1.2	71.4	1.7

values for the total gamma absorbed dose rates, and for the cosmic and terrestrial radiation contributions for each island are shown in Table 1. The cosmic radiation contribution was ca. 36.6 nGy·h⁻¹ (ca. 30% of the total gamma absorbed dose rate). The average value of the total absorbed dose rate for the overall of the Western Canary Islands was estimated to ca. 126.7 nGy·h⁻¹.

Figs. 2a, 3a, 4a and 5a show the terrestrial absorbed dose rates and their empirical frequency distribution for each island. The data fits well to a log-normal distribution, except for El Hierro island, where a quasi-normal distribution is observed. Accordingly, geometric mean values will be used herein.

The spatial distribution of the terrestrial gamma absorbed dose rates is well linked with the geological setting of each island and with the natural radionuclides content of rocks and soils (Figs. 2 to 5). Areas of high terrestrial gamma absorbed dose rates in Tenerife (100–225

nGy·h⁻¹) were located at the center, south and north of the island, related with the volcanism associated with Teide-Pico Viejo complex and Las Cañadas edifice, where felsic rocks (as trachytic and phonolitic lavas and domes, and pyroclastic flow deposits) are more abundant.

In La Palma, higher values (70–130 nGy·h⁻¹) were found mostly in the southeastern part of the Cumbre Vieja ridge, an area where phonotephritic and phonolitic rocks are relatively frequent. Interestingly, the observed gamma absorbed dose rate spatial distribution also coincides with a previously published radon anomalies pattern around Cumbre Vieja complex (Martín et al., 2003).

La Gomera and El Hierro presented the lowest terrestrial gamma absorbed dose rates of the Western Canaries, ranging from 17 to 94 nGy·h⁻¹, and with a relatively uniform spatial distribution, in correspondence with the monotonous basaltic nature of these islands. Just one exception of this behavior was observed in the north of La Gomera

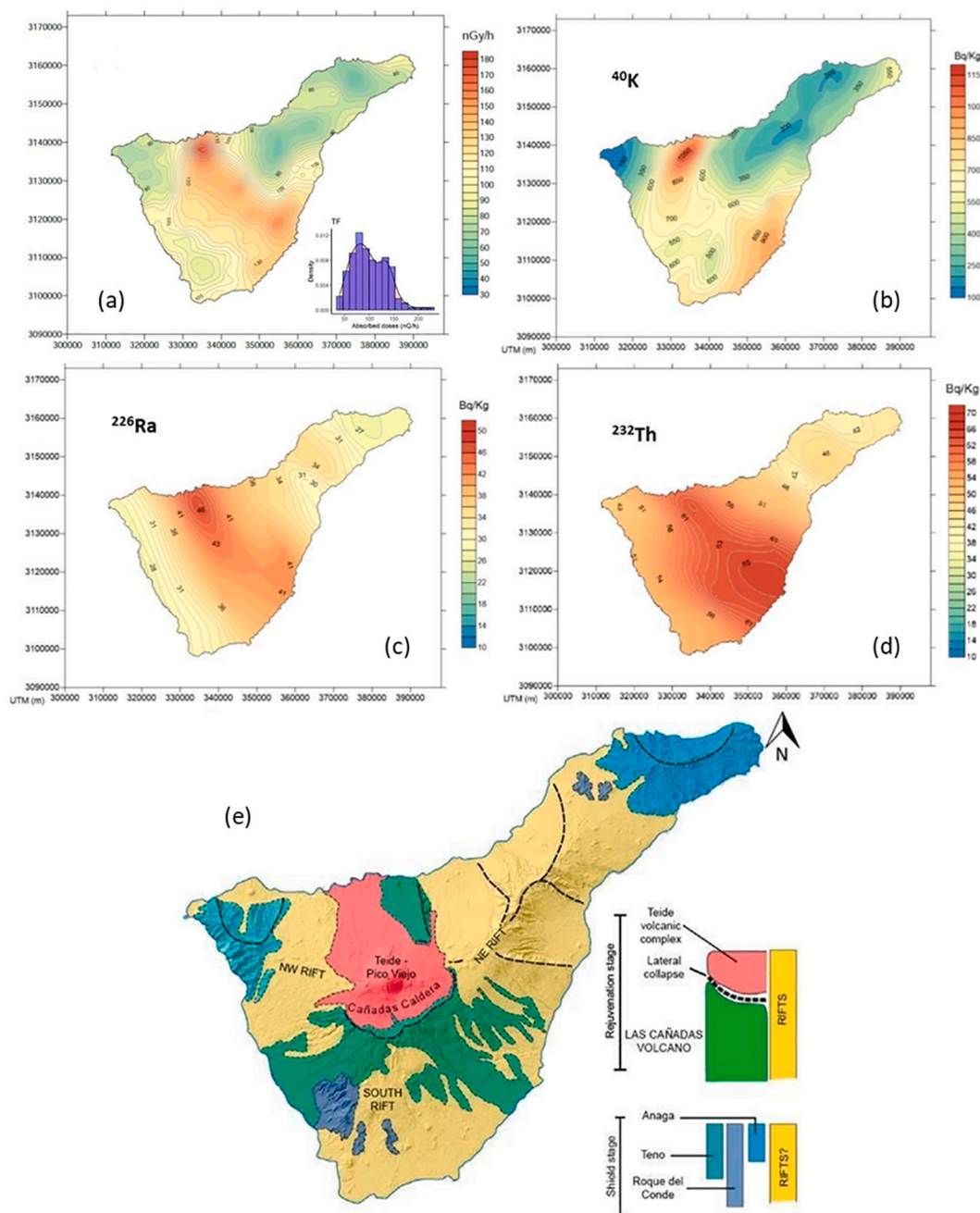


Fig. 2. Terrestrial gamma absorbed dose rate contour map and histogram (a), spatial distribution of ⁴⁰K (b), ²²⁶Ra (c) and ²³²Th (d) activity concentrations in soils and (e) simplified geological map (modified from Troll and Carracedo, 2016) for Tenerife Island.

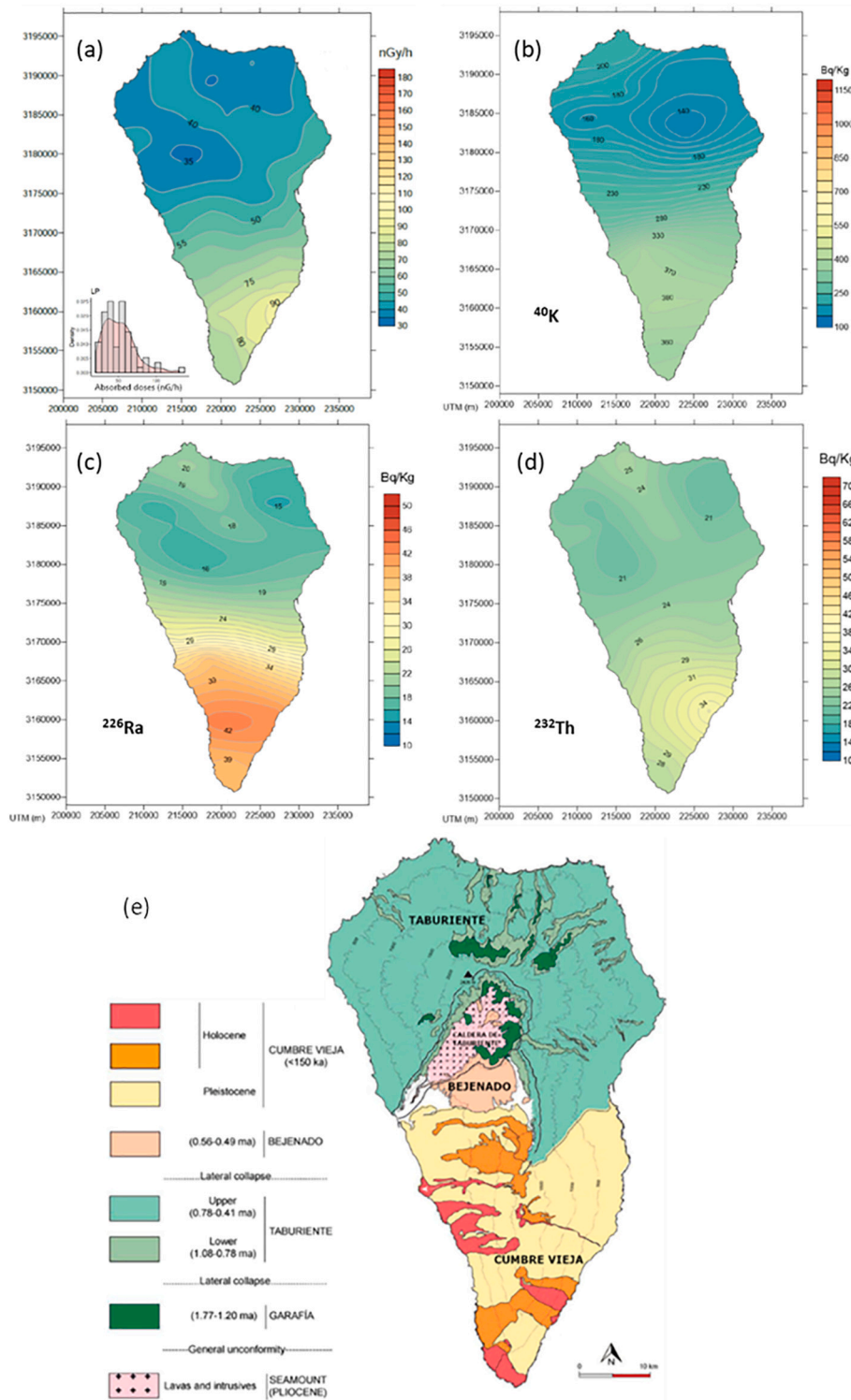


Fig. 3. Terrestrial gamma absorbed dose rate contour map and histogram (a), spatial distribution of ⁴⁰K (b), ²²⁶Ra (c) and ²³²Th (d) activity concentrations in soils and (e) simplified geological map (modified from Troll and Carracedo, 2016) for La Palma Island.

(Vallehermoso municipality), where a relatively high value of ca. 156 nGy·h⁻¹ was found related to the Trachytic-Phonolitic Complex cropping out in this area.

To contextualize our results, we compared the averaged terrestrial absorbed dose rates measured in this work (71.4 ± 1.7 nGy·h⁻¹) with the previously published values for the eastern islands of the archipelago and for other worldwide volcanic regions (Abba et al., 2017; Alomari et al., 2019; Arnedo et al., 2017; Belyaeva et al., 2019; Cinelli et al.,

2020; Minato, 2002; Moreno et al., 2014; Ngachin et al., 2008; Pascholati et al., 1997; Saleh et al., 2011; Tzortzis et al., 2003; UNSCEAR, 2000) (for detail see Table 2). Overall, lower absorbed dose rates (7.4–112 nGy·h⁻¹) are observed in areas where mafic rocks prevail, as in the Western Canary Islands, Mount Cameroon, La Garrotxa, Cyprus or Yemen, meanwhile higher values (110–271 nGy·h⁻¹) are obtained at areas where felsic rocks (phonolites, rhyolites, granites, granodiorites, monzonites) dominate. Considering the volcanic province

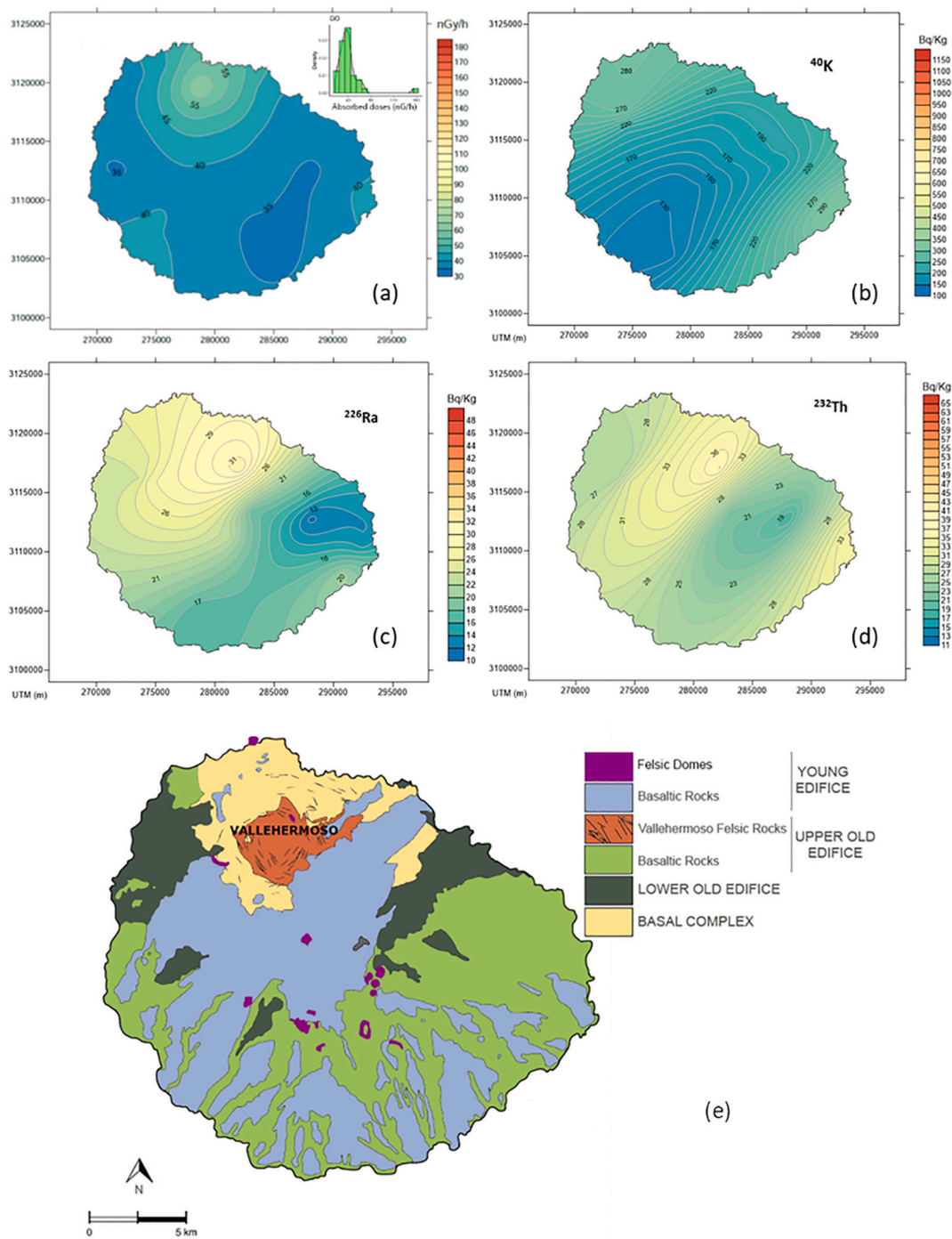


Fig. 4. Terrestrial gamma absorbed dose rate contour map and histogram (a), spatial distribution of ^{40}K (b), ^{226}Ra (c) and ^{232}Th (d) activity concentrations in soils and (e) simplified geological map (modified from Ancochea et al., 2006) for La Gomera Island.

of Canary Islands as a whole, the average terrestrial absorbed dose rate ($57 \text{ nGy}\cdot\text{h}^{-1}$) is similar to the world average value ($59 \text{ nGy}\cdot\text{h}^{-1}$) reported in (UNSCEAR, 2000).

4.2. Concentrations of natural gamma-emitting radionuclides in soils

In the Canary Islands, igneous rocks display a large compositional range, with alkali basalts and basanites as the most common rock types, though trachytes and phonolites are also very abundant, especially in Gran Canaria and Tenerife (Gurenko et al., 2009; Hoernle and Schmincke, 1993; Schmincke, 1982). From a radiological point of view, basic rocks (basanites, nephelinites, tholeiitic and alkali basalts) contain

low concentrations of unstable elements and therefore have very low radioactivity (Schön, 2011). On the other hand, felsic rocks (trachytes, phonolites and peralkaline rhyolites) and intermediate rocks contain higher concentrations of radioactive elements such as ^{40}K , ^{226}Ra , ^{232}Th and ^{238}U , and thus, exhibit higher radiological activity compared to basic and ultrabasic ones (Faure and Mensing, 2005). ^{40}K constitutes 0.012% of total potassium (Webb, 1988), which in turn, is progressively concentrated during magmatic fractionation, thus enriched in felsic relative to mafic rocks. Concerning uranium and thorium, their concentrations are comparatively small, but are also enriched by fractional crystallization into the more silica-rich products. For example, the average concentration of uranium and thorium in syenites is 3.0 and 13

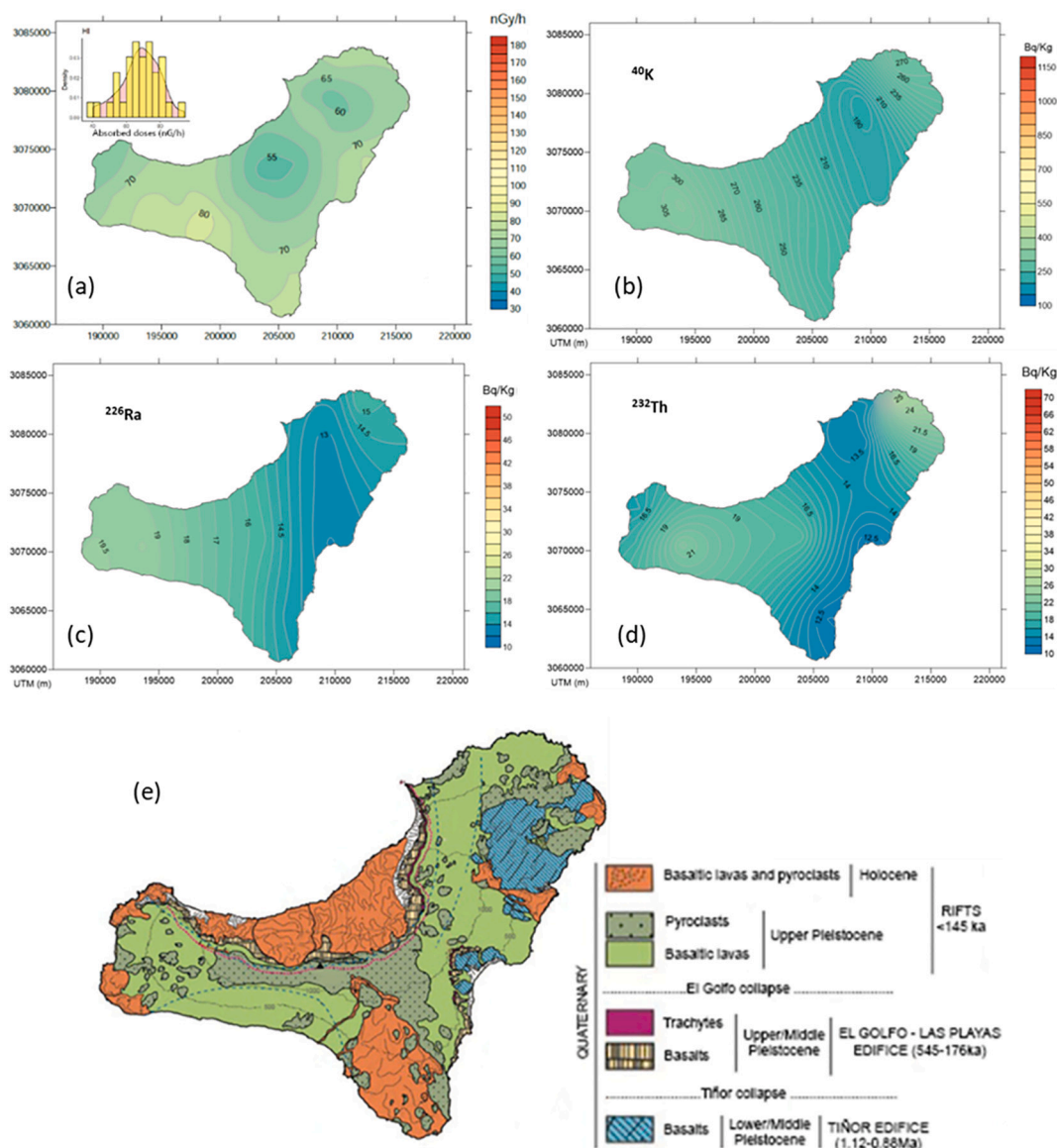


Fig. 5. Terrestrial gamma absorbed dose rate contour map and histogram (a), spatial distribution of ^{40}K (b), ^{226}Ra (c) and ^{232}Th (d) activity concentrations in soils and (e) simplified geological map (modified from Troll and Carracedo, 2016) for El Hierro Island.

ppm respectively, in basalts is 1.0 and 4.0 ppm, and in ultramafic rocks, 0.001 and 0.004 ppm, respectively (Faure and Mensing, 2005).

Table SM1 shows the geometric mean, maximum, minimum and geometric standard deviation values of ^{40}K , ^{226}Ra and ^{232}Th activity concentrations measured in soils from each of the islands. Tenerife presents not only the highest values but also the highest variance. This is in agreement with the large geochemical range of the rock units existing on this island. These results are comparable to those recently published by (Arnedo et al., 2017) for the Eastern Canary Islands.

Contour maps of ^{40}K , ^{226}Ra and ^{232}Th activity concentrations in soils were elaborated using kriging interpolation (see Figs. 2 to 5) and are commented in the following sections. Overall, the spatial distribution of activity concentration of the reported natural radionuclides is reasonably and qualitatively well linked with the main geological features of each island.

4.2.1. Natural gamma radionuclides in Tenerife

Fig. 2 shows the contour maps of natural radionuclides (^{40}K , ^{226}Ra and ^{232}Th), and a simplified geological map for Tenerife. The spatial distribution of ^{40}K , ^{226}Ra and ^{232}Th activity concentrations displayed

the highest values ($>600 \text{ Bq}\cdot\text{kg}^{-1}$, $>40 \text{ Bq}\cdot\text{kg}^{-1}$ and $> 50 \text{ Bq}\cdot\text{kg}^{-1}$, respectively) in the central, southern and northern sectors of the island. Higher values are observed in areas of intermediate and felsic rocks (phonolites and trachytes) corresponding to the Teide-Pico Viejo complex (at the central and northern part of the island) and Las Cañadas edifice (composed mainly by trachytic and phonolitic lavas and domes, and by large pyroclastic flow deposits). Lower soil ^{40}K , ^{226}Ra and ^{232}Th activity concentrations were measured in the oldest basaltic shield outcrops (Teno, Roque del Conde and Anaga massifs) and along the NE ridge, also of basaltic composition.

4.2.2. Natural gamma radionuclides in La Palma

On average, La Palma presented lower activity concentration values than Tenerife for all the natural radioisotopes (see Table SM1). Lower activity values of ^{40}K , ^{226}Ra and ^{232}Th radionuclides ($<200 \text{ Bq}\cdot\text{kg}^{-1}$, $<20 \text{ Bq}\cdot\text{kg}^{-1}$ and $< 25 \text{ Bq}\cdot\text{kg}^{-1}$ respectively) were found in the north (Fig. 3), associated with Cumbre Nueva and Taburiente basaltic volcanism (oldest shield stage), with basic and ultrabasic rock outcrops (basanites and alkali basalts). Higher ^{40}K , ^{226}Ra and ^{232}Th activity concentrations ($300\text{--}500 \text{ Bq}\cdot\text{kg}^{-1}$, $20\text{--}50 \text{ Bq}\cdot\text{kg}^{-1}$ and $25\text{--}45 \text{ Bq}\cdot\text{kg}^{-1}$,

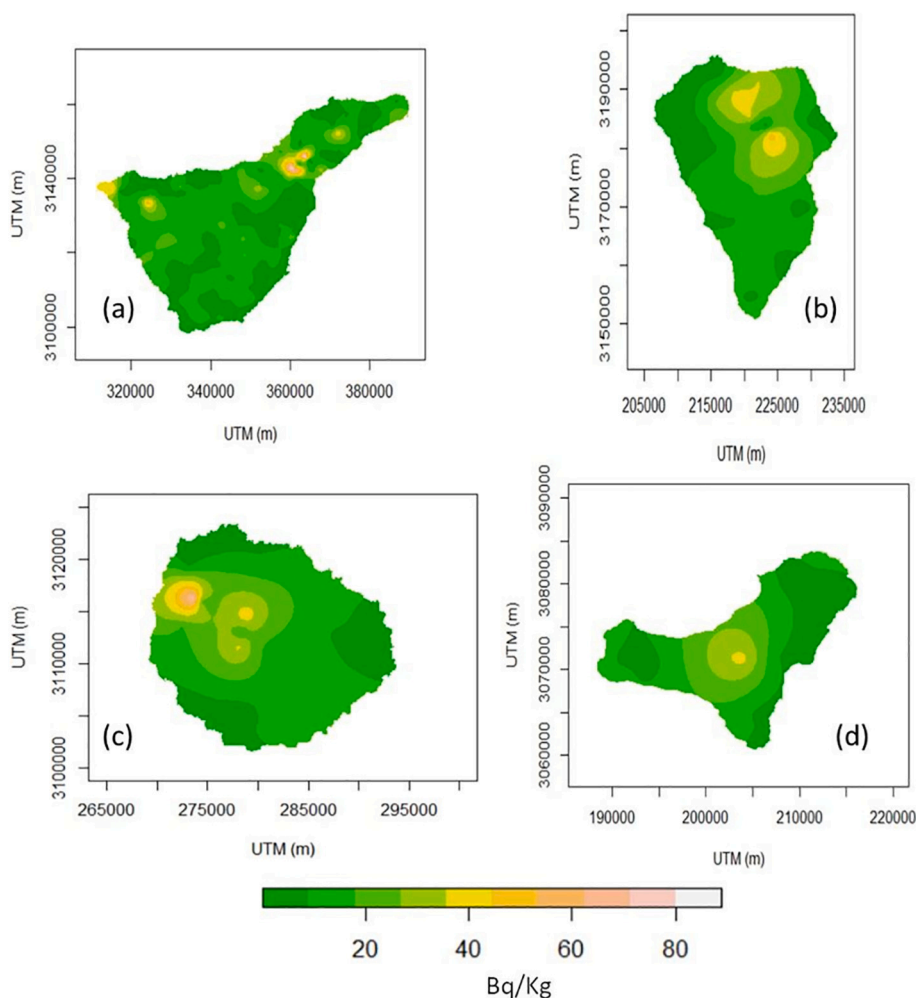


Fig. 6. Spatial distribution[†] of ^{137}Cs activity concentrations on soil samples collected in (a) Tenerife, (b) La Palma, (c) La Gomera and (d) El Hierro islands. [†]Data representation corresponding to the two field surveys (1991 and 2013). The data from 1991 was corrected for decay using a factor of 0.6 (see above).

respectively) were found in the southern part of the island, associated with the recent Cumbre Vieja edifice, where more differentiated lavas (phonotephrites to phonolites) and phonolitic plugs are relatively abundant.

4.2.3. Natural gamma radionuclides in La Gomera

The spatial distribution of all radioisotopes in this island was relatively uniform (Fig. 4) and showed low activity concentrations (see Table SM1), especially for ^{40}K ($177\text{ Bq}\cdot\text{kg}^{-1}$) with values in the range of $50\text{--}450\text{ Bq}\cdot\text{kg}^{-1}$, in coherence with the mostly basaltic nature of La Gomera. Only slightly high ^{226}Ra ($25\text{--}40\text{ Bq}\cdot\text{kg}^{-1}$) and ^{232}Th ($30\text{--}50\text{ Bq}\cdot\text{kg}^{-1}$) activity concentrations values were found to the north, at the Vallehermoso area, spatially associated with the existence of a Trachytic-Phonolitic Complex (Ancochea et al., 2006).

4.2.4. Natural gamma radionuclides in El Hierro

^{40}K , ^{226}Ra and ^{232}Th activity concentrations in soils of El Hierro, the youngest island in the archipelago (<1 Ma), were low and uniform (Fig. 5), even with lower activity and variability than those measured in La Palma and in La Gomera (see Table SM1). The ^{40}K activity concentrations were found in the range of $120\text{--}360\text{ Bq}\cdot\text{kg}^{-1}$ and presented lower variation in comparison with the other three islands. Similar results were found for ^{226}Ra and ^{232}Th , with activity concentrations values in the range of $5\text{--}25\text{ Bq}\cdot\text{kg}^{-1}$ and $10\text{--}35\text{ Bq}\cdot\text{kg}^{-1}$, respectively. These low activity concentrations values, and their spatial distribution, are in correspondence with the geology of the island, where most of the rocks

are of mafic composition.

4.3. Activity concentrations of ^{137}Cs in soils

In this section, the ^{137}Cs activity concentrations measured in soil samples collected at two different surveys, performed in 1991 and 2013, are discussed. The average concentration, the geometric mean and the maximum and minimum values recorded (in $\text{Bq}\cdot\text{kg}^{-1}$) are presented in Table 3. The data from 1991 was multiplied by a factor of 0.6 to correct for the radioactive decay (22 years gap). Box-and-whisker plots of ^{137}Cs activity concentrations in 131 and 121 soil samples collected in 1991 and 2013, respectively, are also provided for each of the islands (Fig. SM2).

Despite the 22 years gap between the two field surveys, the measured activity concentrations of ^{137}Cs were rather similar. Activity concentrations ranged from 1.5 to $100.9\text{ Bq}\cdot\text{kg}^{-1}$ in the data collected in 1991 and from 0.08 to $88.85\text{ Bq}\cdot\text{kg}^{-1}$ in the data collected in 2013 (see Table 3). Thus, the data collected after 22 years does not show a decrease in maximum value. Although, this could be an artifact caused by the discrete sampling used in of our study, we believe that regular atmospheric deposition of ^{137}Cs , produced by dust intrusions from the Saharan desert, are the cause for this effect. A discussion related to this latter hypothesis follows below.

Much of the ^{137}Cs from nuclear weapons testing has now decayed. Areal activity in soils are conventionally expressed in $\text{Bq}\cdot\text{m}^{-2}$ and decay-corrected to a given reference date for comparison. The bomb-derived

Table 2
Terrestrial gamma absorbed dose rates in air at 1 m above volcanic and plutonic rocks.

Location/ Country	Lithology	Terrestrial absorbed dose rate (nGy/h)	Reference
Western Canary Islands (Spain)	Basaltic and felsic volcanic rocks	71.4	This work
Eastern Canary Islands (Spain)	Basaltic (predominant) and felsic volcanic rocks	43	(Arnedo et al., 2017)
Mount Cameroon (Cameroon)	Basalts	29 (*)	(Ngachin et al., 2008)
La Garrotxa (Spain)	Basanites and basalts	51	(Moreno et al., 2014)
Kajaran, Armenia	Monzonites, granites and granodiorites	114.4 (*)	(Belyaeva et al., 2019)
Cyprus	Ophiolite complex (mafic rocks)	7.4 (*)	(Tzortzis et al., 2003)
Japan	Felsic intrusives	110	(Minato, 2002)
	Felsic extrusives	94	
	Mafic rocks	21	
Jordan	Precambrian granitic complex	137 (**)	(Alomari et al., 2019)
Euganean Hills, (Italy)	Volcanic submarine mafic lavas, breccias, hyaloclastites, lavas (intermediate to acidic) and sub-volcanic laccoliths	50.4	(Cinelli et al., 2020)
Itu, Sao Paulo (Brasil)	Granites	145 (*)	(Pascholati et al., 1997)
Jos Plateau (Nigeria)	Older granites	177 (*)	(Abba et al., 2017)
	Younger granites	271 (*)	
	Rhyolites	191 (*)	
	Older basalts	112 (*)	
North Sana'a (Yemen)	Quaternary intraplate volcanism (basalts and trachybasalts)	38.4 (*)	(Saleh et al., 2011)
World average		59	(UNSCEAR, 2000)

(*) Calculated from the concentration of radionuclides. (**) Total gamma absorbed dose rate.

^{137}Cs fallout areal activity estimated by the UNSCEAR (UNSCEAR, 1982) for the northern hemisphere (20° - 30° latitude band) is approximately $1.3 \text{ kBq}\cdot\text{m}^{-2}$ (normalised to 2013). Nuclear reactor waste and accidental releases are the main sources of ^{137}Cs in the current environment (Ashraf et al., 2014; Meusburger et al., 2020; Aoyama, 2018; Evangelidou et al., 2013). The dispersion models published for the

Chernobyl ^{137}Cs (De Cort et al., 1998; <https://www.irsn.fr/EN/publications/thematic-safety/chernobyl/Pages/The-Chernobyl-Plume.aspx>) do not indicate that the study area was impacted directly by this accident. ^{137}Cs detected in air samples after the Fukushima accident at this site were too low (López-Pérez et al., 2013) to significantly impact the concentration of this radionuclide in the soils at this site. However, relatively high ^{137}Cs areal activities, up to $11 \text{ kBq}\cdot\text{m}^{-2}$ (considering only the 2013 data and an average soil density of $900 \text{ kg}\cdot\text{m}^{-3}$), have been reported for the island of Tenerife in this study. Moreover, data from 9 soil samples collected in ravines located in the island of Tenerife in the year 2000 (Hernández Suárez, 2002) also showed high values of up to $6.5 \text{ kBq}\cdot\text{m}^{-2}$. The maximum ^{137}Cs areal activity reported for Tenerife ($11 \text{ kBq}\cdot\text{m}^{-2}$) in this work is comparable to the values reported for Austria ($16 \text{ kBq}\cdot\text{m}^{-2}$) by (Bossey et al., 2001) and higher than the values reported for the Spain mainland ($1.5 \text{ kBq}\cdot\text{m}^{-2}$) by (Caro et al., 2013) as well as European top-soils ($2.1 \text{ kBq}\cdot\text{m}^{-2}$) by (Meusburger et al., 2020). The values above were all normalised to 2013.

To understand the data reported above, we must consider other potential sources contributing to this radionuclide activity in soils at the study area. Dust particles from the Sahara Desert are often deposited over the islands (Alonso-Pérez et al., 2007; Goudie and Middleton, 2001). It is known that aerosols may travel at distances depending on two main factors: wind speed and particle size distribution. At the source, i.e. the desert, a mixture of coarse and fine particles are continuously mixed at ground level by turbulence under the effect of intense overheating and consequent strong thermal convection. Mineral particles are conveyed away possibly with ^{40}K transported within the crystal lattice of the coarse mineral fraction and ^{137}Cs associated to the clay component, which is always present in Saharan dust. This might reasonably explain the simultaneous increase of both radionuclides during deposition events reported by (Hernandez et al., 2007; Karlsson et al., 2008; López-Pérez et al., 2020). Similar effects have been reported for other sites affected by seasonal dust storms. For example, (Akata et al., 2007) studied the atmospheric deposition of ^{137}Cs in Rakkasho, Japan and its relationship with Asian dust events. These authors found the southern regions of Mongolia and northeast China as important sources of ^{137}Cs to their site of study. (Fukuyama and Fujiwara, 2008) found that the deposition of ^{137}Cs from a single Asian dust event was $62.3 \text{ mBq}\cdot\text{m}^{-2}$ and accounted for 67% of the total ^{137}Cs deposition during their entire monitoring period. (Hamadneh et al., 2015) studied the radioactivity of seasonal dust storms in the Middle East. The average activity concentration of fallout ^{137}Cs (17.0 Bq/kg) was larger than that found in soil (2.3 Bq/kg). Recently, (Aba et al., 2018) studied the atmospheric deposition fluxes of ^{137}Cs associated with dust fallout in the north-eastern Arabian Gulf and found an average annual atmospheric deposition flux of ^{137}Cs of $4.3 \text{ Bq}\cdot\text{m}^{-2}$, with a wide range of values. The

Table 3

^{137}Cs activity concentrations (average, geometric mean, maximum and minimum) in soils of Tenerife (TF), El Hierro (HI), La Palma (LP) and La Gomera (GO) islands measured in two different surveys (in $\text{Bq}\cdot\text{kg}^{-1}$). (n) represents the number of sampling points and (%) is the percentage of soil samples with concentrations above the MDA.

Island	year	n	%	Average $\text{Bq}\cdot\text{kg}^{-1}$	Geometric mean $\text{Bq}\cdot\text{kg}^{-1}$	Minimum $\text{Bq}\cdot\text{kg}^{-1}$	Maximum $\text{Bq}\cdot\text{kg}^{-1}$
TF	1991			18.2	12.8	1.50	101
	decay	103	70	10.9	7.68	0.901	60.5
	2013	73	95	9.52	3.74	0.313	88.9
LP	1991			20.6	17.8	6.50	52.4
	decay	12	83	12.4	10.7	3.90	31.4
	2013	25	100	13.0	6.57	0.52	49.1
GO	1991			19.7	13.8	2.70	68.8
	decay	10	100	11.8	8.29	1.62	41.3
	2013	13	69	17.5	4.64	0.31	74.7
HI	1991			12.9	12.7	10.1	16.0
	decay	6	67	7.76	7.64	6.30	9.60
	2013	10	90	7.37	1.53	0.080	38.4

^{137}Cs maps for the 4 studied islands, (Fig. 6), have been generated with the combined data from the two field surveys. This was possible because of the good spatial agreement of the two data sets. The data presented in Fig. 6 are normalised to 2013.

extreme values extended to approximately $50 \text{ Bq}\cdot\text{m}^{-2}$ for ^{137}Cs and were associated with the dust storm that hit Kuwait in March 2011.

The enrichment factor of ^{137}Cs in the soils at this site cannot be extrapolated from the data available from air filters because there are numerous factors (aerosol size, precipitation, altitude, soil permeability, infiltration, organic matter content, vegetation, erosion, etc.) that may influence both the atmospheric deposition and the accumulation rate in soils. Direct deposition measurements during dust intrusion events are necessary.

The determination of $^{239+240}\text{Pu}$ in soils and aerosol filters may help to determine whether the ^{137}Cs in the Saharan dust may be related to the French nuclear weapon tests performed in Algeria (García-Tenorio, 2018; Menut et al., 2009) or from the ^{137}Cs deposited after the Chernobyl accident. ^{90}Sr and ^{241}Am , have been reported in water and soil samples collected in the island of Tenerife (Hernandez et al., 2007; Hernández Suárez, 2002). Determination of these radionuclides may also help to understand the origin of the source/s of ^{137}Cs .

Many authors report that ^{137}Cs is normally stored in the top 15 cm of soil (Malins et al., 2016; Matsuda et al., 2015), the same depth sampled in 2013. However, we cannot be certain that our latest data fully reflects the complete areal activity of this radionuclide at all sampling sites. Soil samples collected at 0, 30 and 60 cm depth in 1998 (Fernández de Aldecoa, 2000) showed that, although 90% of the activity was located in the top 15 cm, measurable concentrations were still found below 30 cm. A different sampling strategy (vertical profiles) will be used in future studies to allow the study of key processes controlling the accumulation and distribution of ^{137}Cs in soil samples.

4.4. Comparison between soil radionuclide concentrations and terrestrial absorbed dose rates in air

In this section we study the correlation between the terrestrial gamma absorbed dose rates and the radionuclides concentrations measured in soil samples. Spearman's correlation coefficients are shown in Table 4. Terrestrial absorbed dose rate showed a high correlation ($0.79, p < 0.01$) with ^{40}K activity concentration, while such correlation was moderate for the other two radionuclides. Interestingly, ^{226}Ra and ^{232}Th presented a high correlation of about 0.82 ($p < 0.01$). Similar results have been previously reported by other authors (Jakhu et al., 2018; Kovács et al., 2013). ^{137}Cs did not show any significant correlation with other radionuclides and the terrestrial absorbed dose rates. Such findings can be justified in terms of the different origin of this radionuclide, since it is not related to the geological and geochemical composition of the volcanic soils in the studied areas.

Based on the correlation analysis, a Multiple Regression Analysis (MRA) was done on the full dataset to estimate the terrestrial absorbed dose based on the radionuclide concentrations in soils (^{40}K , ^{226}Ra , and ^{232}Th). MRA confirmed our initial results. Only the ^{40}K contribution was statistically significant ($p < 0.01$). The obtained linear model: terrestrial absorbed dose (nGy/h) = $40.6 + 0.09 [^{40}\text{K}]$ (Bq/kg) presented an adjusted r-squared value of about 0.54. Therefore, such a simple linear model could explain ca. 54% of the total variance of the terrestrial absorbed dose rates dataset.

Principal Components Analysis (PCA) was used to identify and assess

Table 4
Correlation (Spearman's method) between terrestrial absorbed dose rate and radionuclide activity concentrations in soils of the Western Canary Islands.

	^{40}K	^{226}Ra	^{232}Th	^{137}Cs	TADR
^{40}K	1				
^{226}Ra	0.68	1			
^{232}Th	0.67	0.82	1		
^{137}Cs	-0.27	0	-0.14	1	
TADR ^a	0.79	0.64	0.66	-0.17	1

Bold is used to mark moderate and strong (correlations coefficients < 0.6).

^a TADR: Terrestrial absorbed dose rate.

the contribution of each radionuclide to the terrestrial absorbed dose. Results obtained for the rotated factor loadings for each variable are presented in Table 5. The first two principal components explained ca. 83% of the total dataset variance. After rotation based on the Varimax method, the first rotated component (RC1) explained ca. 64.7% of the total variance. Values for RC1, listed in Table 5, showed a positive correlation with ^{40}K (0.90), ^{226}Ra (0.86), ^{232}Th (0.89) and the terrestrial absorbed dose (0.87). This component may be putatively assigned to the contribution of naturally occurring radionuclides to the absorbed dose rates. The second rotated component (RC2) explained ca. 18% of the total variance and is determined by high positive loadings with ^{137}Cs . Therefore, we defined this component as an artificial contribution to the terrestrial absorbed dose rates. Based on these results we conclude that the main contribution to the absorbed dose is due to the natural radionuclides found in the RC1 component. This conclusion is in good agreement with the minimal contribution due to the fallout (see previous section) and that among the main factors affecting the terrestrial absorbed dose are the underlying geological features and geochemical composition of the volcanic soils.

Based on the Beck's equation for natural radionuclides (Hassan et al., 2018; Huang et al., 2016) (see Eq. (2)):

$$\text{TADR} (\text{nGy}/\text{h}) = 0.0417 \cdot C_{40\text{K}} + 0.462 \cdot C_{226\text{Ra}} + 0.604 \cdot C_{232\text{Th}} \quad (2)$$

where TADR, $C_{40\text{K}}$, $C_{226\text{Ra}}$ and $C_{232\text{Th}}$ are the terrestrial absorbed dose rates and the activity concentrations in the bedrock in $\text{Bq}\cdot\text{kg}^{-1}$ of ^{40}K , ^{226}Ra and ^{232}Th , respectively. Using an additional Dose Rate conversion Factor (DRF) for ^{137}Cs ($0.2 \text{ nSv}\cdot\text{h}^{-1}/\text{Bq}\cdot\text{kg}^{-1}$) (Fernández de Aldecoa, 2000) and the conversion factor $1.2 \text{ Gy}/\text{Sv}$, we estimated the total contribution of the analysed radionuclides in the Western Canary Islands (Fig. 7). A 99% of the observed absorbed dose rate is explained by the natural radionuclides, being the main contribution due to ^{40}K with ca. 83%. The effect due to artificial radionuclides i.e., ^{137}Cs is minimal and only represents about 1% of the absorbed dose. Nevertheless, in some of the studied sites, with high ^{137}Cs activity concentrations (ca. 100 $\text{Bq}\cdot\text{kg}^{-1}$), its contribution can reach values of $20 \text{ nGy}\cdot\text{h}^{-1}$ (representing ca. 35–50% of the total contribution).

Finally, and based on the radionuclide activity concentration in soils, we calculated the annual effective dose received by the inhabitants of the western Canary Islands due to the terrestrial contribution. This value was estimated to be ca. $0.37 \text{ mSv}\cdot\text{year}^{-1}$, representing ca. 15% of the annual effective dose ($2.4 \text{ mSv}\cdot\text{year}^{-1}$) reported by the UNSCEAR (UNSCEAR, 2008), being in good agreement with the tabulated terrestrial contribution in the literature.

5. Conclusions

In this work, the activities of natural and artificial gamma-emitting radionuclides in soil samples collected in the Western Canary Islands have been studied. The main sites of radiological interest have been identified as shown in the radiometric (terrestrial absorbed dose) maps provided for each of the four studied islands.

In situ outdoor gamma absorbed dose rates (352 sample sites) and

Table 5
Results of the Varimax rotated factor matrix (loadings > 0.6 are marked in bold).

	RC1	RC2
^{40}K	0.901	
^{226}Ra	0.861	0.141
^{232}Th	0.889	0.141
^{137}Cs	0.371	0.924
Terrestrial absorbed dose	0.867	
Eigenvalue	3.233	0.909
Variance explained	0.647	0.182
Total Variance explained	0.647	0.828

RC = Rotated Component.

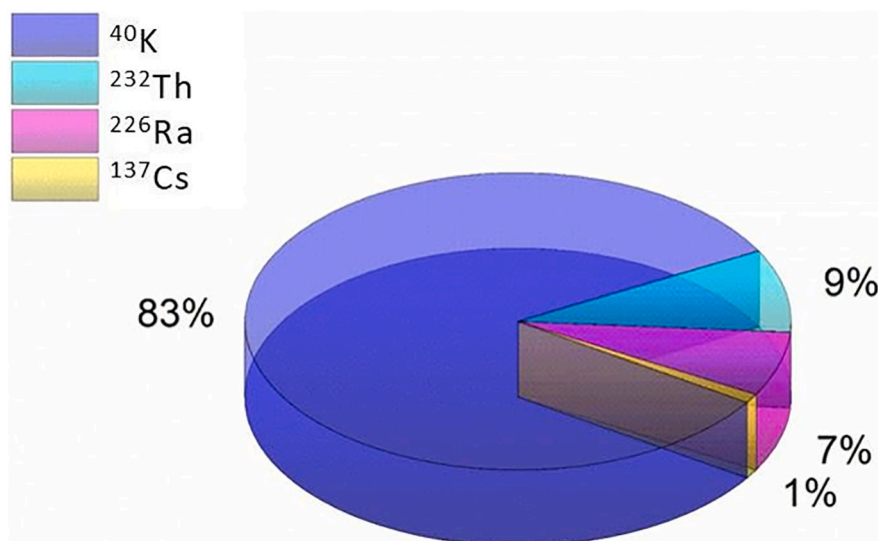


Fig. 7. Estimated contributions of each radionuclide to the absorbed dose rates in the Western Canary Islands.

radiometric determinations of ^{40}K , ^{226}Ra and ^{232}Th in soils (121 samples in the 2013 field survey) were obtained and compared for this purpose. The spatial distribution of terrestrial gamma absorbed dose rates and activity concentrations of ^{40}K , ^{226}Ra and ^{232}Th were, in general, robustly related with the main geological features of each island. Their ranges (17.2–225.3 $\text{nGy}\cdot\text{h}^{-1}$, and 52.0–1240.1, 7.0–71.0, 8.1–147.5 $\text{Bq}\cdot\text{kg}^{-1}$ of ^{40}K , ^{226}Ra and ^{232}Th , respectively) were like those reported for the eastern islands of this archipelago and close to the average world values. The highest values for both, absorbed doses and radionuclide activities, were measured at Tenerife, associated with areas of intermediate and felsic rocks (phonolites and trachytes) in the Teide-Pico Viejo complex and Las Cañadas edifice (at the central and northern part of the island).

The spatial distribution of ^{137}Cs activity concentrations in the soils of these islands, at two different moments in time (1991 and 2013), has also been reported here. The assessment of the distribution of this man-made radionuclide is a key contribution of this work with application for planning future radioecological studies in this oceanic region. Values ranged between 0.08 and 88.85 $\text{Bq}\cdot\text{kg}^{-1}$ and were estimated to correspond to areal activities of up to 11 $\text{kBq}\cdot\text{m}^{-2}$ (based solely on data from the 2013 survey). This is higher than expected from the global fallout in this region. It is, therefore, important to identify the various sources of this radionuclide at the studied sites to enhance our understanding of the radiological hazard produced by this man-made radionuclide. An enrichment process in the top layers of soil produced by the contributions of ^{137}Cs brought to the islands by Saharan dust intrusions is, most likely, the cause for the observed high concentrations. This enrichment process will be studied in more detail in the future.

In terms of radiological risk, the levels of gamma absorbed doses reported here pose no risk to the local population. However, the extensive results obtained will serve as a baseline for future environmental radioactivity studies, especially those addressing the impact of atmospheric sources of ^{137}Cs upon the inhabitants of the archipelago.

CRedit authorship contribution statement

María López-Pérez: Methodology, Investigation, Formal analysis, Writing – original draft, Visualization. **Candelaria Martín-Luis:** Writing – original draft, Visualization. **Francisco Hernández:** Writing – original draft, Visualization. **Esperanza Liger:** Writing – original draft, Visualization. **José Carlos Fernández-Aldecoa:** Methodology, Investigation, Resources. **José Miguel Lorenzo-Salazar:** Writing – original draft, Visualization. **José Hernández-Armas:** Conceptualization, Funding acquisition, Investigation, Resources. **Pedro A. Salazar-Carballo:**

Formal analysis, Writing – original draft, Visualization, Supervision.

Declaration of competing interest

The authors declare that they have no known competing financial interests or personal relationships that could have appeared to influence the work reported in this paper.

Acknowledgements

This work has been financially supported by the Spanish Nuclear Safety Council (CSN).

Appendix A. Supplementary data

Supplementary data to this article can be found online at <https://doi.org/10.1016/j.gexplo.2021.106840>.

References

- Aba, A., Al-Dousari, A.M., Ismaeel, A., 2018. Atmospheric deposition fluxes of ^{137}Cs associated with dust fallout in the northeastern Arabian Gulf. *J. Environ. Radioact.* 192, 565–572.
- Abba, H.T., Hassan, W.M.S.W., Saleh, M.A., Aliyu, A.S., Ramli, A.T., 2017. Estimation of Terrestrial gamma radiation (TGR) dose rate in characteristic geological formations of Jos Plateau, Nigeria. *Malays. J. Fundam. Appl. Sci.* 13, 593–597.
- Akata, N., Hasegawa, H., Kawabata, H., Chikuchi, Y., Sato, T., Ohtsuka, Y., Kondo, K., Hisamatsu, S.i., 2007. Deposition of ^{137}Cs in Rokkasho, Japan and its relation to Asian dust. *J. Environ. Radioact.* 95, 1–9.
- Alomari, A.H., Saleh, M.A., Hashim, S., Alsayaheen, A., 2019. Investigation of natural gamma radiation dose rate (GDR) levels and its relationship with soil type and underlying geological formations in Jordan. *J. Afr. Earth Sci.* 155, 32–42.
- Alonso-Pérez, S., Cuevas, E., Querol, X., Viana, M., Guerra, J.C., 2007. Impact of the Saharan dust outbreaks on the ambient levels of total suspended particles (TSP) in the marine boundary layer (MBL) of the Subtropical Eastern North Atlantic Ocean. *Atmos. Environ.* 41, 9468–9480.
- Anagnostakis, M.J., 2015. Environmental radioactivity measurements and applications – difficulties, current status and future trends. *Radiat. Phys. Chem.* 116, 3–7.
- Ancochea, E., Hernán, F., Huertas, M.J., Brändle, J.L., Herrera, R., 2006. A new chronostratigraphical and evolutionary model for La Gomera: Implications for the overall evolution of the Canary Archipelago. *J. Volcanol. Geotherm. Res.* 157, 271–293.
- Aoyama, M., 2018. Long-range transport of radiocaesium derived from global fallout and the Fukushima accident in the Pacific Ocean since 1953 through 2017—part I: source term and surface transport. *J. Radioanal. Nucl. Chem.* 318, 1519–1542.
- Arnedo, M.A., Rubiano, J.G., Alonso, H., Tejera, A., González, A., González, J., Gil, J.M., Rodríguez, R., Martel, P., Bolívar, J.P., 2017. Mapping natural radioactivity of soils in the eastern Canary Islands. *J. Environ. Radioact.* 166, 242–258.

- Ashraf, M.A., Akib, S., Maah, M.J., Yusoff, I., Balkhair, K.S., 2014. Cesium-137: radiochemistry, fate, and transport, remediation, and future concerns. *Crit. Rev. Environ. Sci. Technol.* 44, 1740–1793.
- Baeza, A., Alonso, A., Heras, M., 2003. Procedimiento para la conservación y preparación de muestras de suelo para la determinación de la radiactividad. In: *Colección Informes Técnicos 11.2003. Serie Vigilancia Radiológica Ambiental Procedimiento 1.2. INT-04-07 Consejo de Seguridad Nuclear, Madrid.*
- Baggoura, B., Noureddine, A., Benkrad, M., 1998. Level of natural and artificial radioactivity in Algeria. *Appl. Radiat. Isot.* 49, 867–873.
- Belyaeva, O., Pyuskyulyan, K., Movsisyan, N., Saghatlyan, A., Carvalho, F.P., 2019. Natural radioactivity in urban soils of mining centers in Armenia: Dose rate and risk assessment. *Chemosphere* 225, 859–870.
- Bossev, P., Ditto, M., Falkner, T., Henrich, E., Kienzl, K., Rappelsberger, U., 2001. Contamination of Austrian soil with caesium-137. *J. Environ. Radioact.* 55, 187–194.
- Caro, A., Legarda, F., Romero, L., Herranz, M., Barrera, M., Valiño, F., Idoeta, R., Olondo, C., 2013. Map on predicted deposition of Cs-137 in Spanish soils from geostatistical analyses. *J. Environ. Radioact.* 115, 53–59.
- Carracedo, J.C., Torrado, F.J.P., Ancochea, E., Meco, J., Hernán, F., Cubas, C.R., Casillas, R., Badiola, E.R., Ahijado, A., Gibbons, W., Moreno, T., 2002. *Cenozoic Volcanism II: The Canary Islands, The Geology of Spain.* Geological Society of London (p. 0).
- Carroll, J., Lerche, I., 2010. Sedimentary radioactive tracers and diffusive models. *J. Environ. Radioact.* 101, 597–600.
- Cartwright, I., Cendón, D., Currell, M., Meredith, K., 2017. A review of radioactive isotopes and other residence time tracers in understanding groundwater recharge: possibilities, challenges, and limitations. *J. Hydrol.* 555, 797–811.
- Cinelli, G., Brattich, E., Coletti, C., De Ingeniis, V., Mazzoli, C., Mostacci, D., Sassi, R., Tositti, L., 2020. Terrestrial gamma dose rate mapping (Euganean Hills, Italy): comparison between field measurements and HPGe gamma spectrometric data. In: *Radiation Effects and Defects in Solids*, 175, pp. 54–67.
- Coello-Bravo, J.J., Márquez, Á., Herrera, R., Huertas, M.J., Ancochea, E., 2020. Multiple related flank collapses on volcanic oceanic islands: evidence from the debris avalanche deposits in the Orotava Valley water galleries (Tenerife, Canary Islands). *J. Volcanol. Geotherm. Res.* 401, 106980.
- De Cort, Dubois, M., D., G., Germenchuk, F., A., M., Janssens, I., Jones, A., N., A., Knaviskova, K., E. & I., M.M., Y.M., N., V.A., P., ED, S., LY, S., YS, T., Tsaturov, 1998. Atlas of Caesium 137 Deposition on Europe After the Chernobyl accident. EUR 1673 EN/RU.
- Evangelou, N., Balkanski, Y., Cozic, A., Möller, A.P., 2013. Global transport and deposition of 137Cs following the Fukushima Nuclear Power Plant accident in Japan: emphasis on Europe and Asia using high-resolution model versions and radiological impact assessment of the human population and the environment using interactive tools. *Environ. Sci. Technol.* 47, 5803–5812.
- Evangelou, N., Hamburger, T., Talerko, N., Zibitso, S., Bondar, Y., Stohl, A., Balkanski, Y., Mousseau, T.A., Möller, A.P., 2016. Reconstructing the Chernobyl Nuclear Power Plant (CNPP) accident 30 years after. A unique database of air concentration and deposition measurements over Europe. *Environ. Pollut.* 216, 408–418.
- Faure, G., Mensing, T.M., 2005. The U-Pb, Th-Pb, and Pb-Pb Methods. In: Faure, G., Mensing, T.M. (Eds.), *Isotopes: Principles and Applications*, Third edition. John Wiley & Sons, Inc., New Jersey, pp. 214–255.
- Fernández de Aldecoa, J.C., 2000. Radiación natural en aire y suelos de las Islas Canarias Occidentales (Tesis Doctoral). Universidad de La Laguna.
- Fernández-Aldecoa, J.C., Robayna, B., Allende, A., Poffijn, A., Hernández-Armas, J., 1992. Natural Radiation in Tenerife (Canary Islands). *Radiat. Prot. Dosim.* 45, 545–548.
- Ferrer, M., de Vallejo, L.G., Seisdedos, J., Coello, J.J., García, J.C., Hernández, L.E., Casillas, R., Martín, C., Rodríguez, J.A., Madeira, J., Andrade, C., Freitas, M.C., Lomoschitz, A., Yepes, J., Meco, J., Betancort, J.F., 2013. Güifmar and La Orotava mega-landslides (Tenerife) and tsunamis deposits in Canary Islands. In: Margottini, C., Canuti, P., Sassa, K. (Eds.), *Landslide Science and Practice, Complex Environment*, vol. 5. Springer, Berlin Heidelberg, Berlin, Heidelberg, pp. 27–33.
- Filgueiras, R.A., Silva, A.X., Ribeiro, F.C.A., Lauria, D.C., Viglio, E.P., 2020. Baseline, mapping and dose estimation of natural radioactivity in soils of the Brazilian state of Alagoas. *Radiat. Phys. Chem.* 167, 108332.
- Fukuyama, T., Fujiwara, H., 2008. Contribution of Asian dust to atmospheric deposition of radioactive cesium (137Cs). *Sci. Total Environ.* 405, 389–395.
- García-Tenorio, R., 2018. 240Pu/239Pu atom ratio as a fingerprint of local and tropospheric fallout due to events involving nuclear weapons: a review. *J. Radiat. Nucl. Appl.* 3, 65–77.
- Goudie, A.S., Middleton, N.J., 2001. Saharan dust storms: nature and consequences. *Earth Sci. Rev.* 56, 179–204.
- Gurenko, A.A., Sobolev, A.V., Hoernle, K.A., Hauff, F., Schmincke, H.-U., 2009. Enriched, HIMU-type peridotite and depleted recycled pyroxenite in the Canary plume: a mixed-up mantle. *Earth Planet. Sci. Lett.* 277, 514–524.
- Hamadneh, H.S., Ababneh, Z.Q., Hamasha, K.M., Ababneh, A.M., 2015. The radioactivity of seasonal dust storms in the Middle East: the May 2012 case study in Jordan. *J. Environ. Radioact.* 140, 65–69.
- Hassan, N.M., Kim, Y.J., Jang, J., Chang, B.U., Chae, J.S., 2018. Comparative study of precise measurements of natural radionuclides and radiation dose using in-situ and laboratory γ -ray spectroscopy techniques. *Scientific REPOrTs* 8, 14115. <https://doi.org/10.1038/s41598-018-32220-9>.
- Hernández Suárez, F.J., 2002. Optimisation of environmental Gamma Spectrometry Using Monte Carlo Methods. Universitat de València, ISBN 91-554-5399-6.
- Hernandez, F., Karlsson, L., Hernandez-Armas, J., 2007. Impact of the tropical storm Delta on the gross alpha, gross beta, 90Sr, 210Pb, 7Be, 40K and 137Cs activities measured in atmospheric aerosol and water samples collected in Tenerife (Canary Islands). *Atmos. Environ.* 41, 4940–4948.
- Hernández-Gutiérrez, L.E., Eff-Darwich, A., Viñas, R., Rodríguez-Losada, J.A., 2011. Radiology of Canarian volcanic rocks. In: *Harmonising Rock Engineering and the Environment.* Taylor & Francis Group.
- Herranz, M., Jiménez, R., Navarro, E., Payeras, J., Pinilla, J., 2003. Procedimiento de toma de muestra para la determinación de la radioactividad en suelos: capa superficial. In: *Colección Informes Técnicos 11.2002. Serie Vigilancia Radiológica Ambiental Procedimiento 1.1. INT-04-07. Consejo de Seguridad Nuclear, Madrid.*
- Hirayama, Y., Okawa, A., Nakamachi, K., Aoyama, T., Okada, Y., Oi, T., Hirose, K., Kikawada, Y., 2020. Estimation of water seepage rate in the active crater lake system of Kusatsu-Shirane volcano, Japan, using FDNPP-derived radioactive cesium as a hydrological tracer. *J. Environ. Radioact.* 218, 106257.
- Hoernle, K., Schmincke, H.-U., 1993. The petrology of the tholeiites through melilite nephelinites on Gran Canaria, Canary Islands: crystal fractionation, accumulation, and depths of melting. *J. Petrol.* 34, 573–597. <https://www.irs.fr/EN/publications/thematic-safety/chernobyl/Pages/The-Chernobyl-Plume.aspx>.
- Huang, Y.J., Guo, G.Y., He, Y., Yang, L.T., Shan, Z., Chen, C.F., Shang-Guan, Z.H., 2016. A comparative study of terrestrial gamma dose rate in air measured by thermoluminescent dosimeter, portable survey meter and HPGe gamma spectrometer. *J. Environ. Radioact.* ISSN: 0265-931X 164, 13–18. <https://doi.org/10.1016/j.jenvrad.2016.06.020>.
- Hunt, J.E., Talling, P.J., Clare, M.A., Jarvis, I., Wynn, R.B., 2014. Long-term (17 Ma) turbidite record of the timing and frequency of large flank collapses of the Canary Islands. *Geochim. Geophys. Geosyst.* 15, 3322–3345.
- Ithiphoonthanakorn, T., Dann, S.E., Crout, N.M.J., Shaw, G., 2019. Nuclear weapons fallout 137Cs in temperate and tropical pine forest soils, 50 years post-deposition. *Sci. Total Environ.* 660, 807–816.
- Jakhu, R., Mehra, R., Bangotra, P., Kaur, K., Mittal, H.M., 2018. Estimation of terrestrial radionuclide concentration and effect of soil parameters on exhalation and emanation rate of radon. *J. Geochem. Explor.* 184, 296–303.
- Karlsson, L., Hernandez, F., Rodríguez, S., López-Pérez, M., Hernandez-Armas, J., Alonso-Pérez, S., Cuevas, E., 2008. Using 137Cs and 40K to identify natural Saharan dust contributions to PM10 concentrations and air quality impairment in the Canary Islands. *Atmos. Environ.* 42, 7034–7042.
- Kovács, T., Szeiler, G., Fábrián, F., Kardos, R., Gregorič, A., Vaupotič, J., 2013. Systematic survey of natural radioactivity of soil in Slovenia. *J. Environ. Radioact.* 122, 70–78.
- López-Pérez, M., Ramos-López, R., Perestelo, N.R., Duarte-Rodríguez, X., Bustos, J.J., Alonso-Pérez, S., Cuevas, E., Hernández-Armas, J., 2013. Arrival of radionuclides released by the Fukushima accident to Tenerife (Canary Islands). *J. Environ. Radioact.* 116, 180–186.
- López-Pérez, M., Lorenzo-Salazar, J.M., Expósito, F.J., Díaz, J.P., Salazar, P., 2020. Impact of a massive dust storm on the gross alpha, gross beta, 40K, 137Cs, 210Pb, 7Be activities measured in atmospheric aerosols collected in Tenerife, Canary Islands. *Atmos. Environ.* 239, 117806.
- Malins, A., Kurikami, H., Nakama, S., Saito, T., Okumura, M., Machida, M., Kitamura, A., 2016. Evaluation of ambient dose equivalent rates influenced by vertical and horizontal distribution of radioactive cesium in soil in Fukushima Prefecture. *J. Environ. Radioact.* 151, 38–49.
- Martin, M., Ahijado, A., Nuez, J., Quesada, M., Steinitz, G., Vulkan, U., Eff-Darwich, A., 2003. Radon survey at La Palma Island (Canary Islands): first results. In: *Vulcanica – Revista Portuguesa de Vulcanologia*, 1, pp. 113–116.
- Matsuda, N., Mikami, S., Shimoura, S., Takahashi, J., Nakano, M., Shimada, K., Uno, K., Hagiwara, S., Saito, K., 2015. Depth profiles of radioactive cesium in soil using a scraper plate over a wide area surrounding the Fukushima Dai-ichi Nuclear Power Plant, Japan. *J. Environ. Radioact.* 139, 427–434.
- Maxwell, O., Olusegun, O.A., Emmanuel, S.J., Jjeh, B.I., Uchechukwu, A.O., Oluwasegun, A., Ogunrinola, E.I., Angbando, M.T.T., Ifeanyi, A.O., Saeed, M.A., 2020. Spatial distribution of gamma radiation dose rates from natural radionuclides and its radiological hazards in sediments along river Iju, Ogun state Nigeria. *MethodsX* 7, 101086.
- McKenzie, T., Dulai, H., 2017. Fukushima-derived radiocesium fallout in Hawaiian soils. *J. Environ. Radioact.* 180, 106–113.
- Menut, L., Masson, O., Bessagnet, B., 2009. Contribution of Saharan dust on radionuclide aerosol activity levels in Europe? The 21–22 February 2004 case study. *J. Geophys. Res. Atmos.* 114.
- Meusburger, K., Evrard, O., Alewell, C., Borrelli, P., Cinelli, G., Ketterer, M., Mabit, L., Panagos, P., van Oost, K., Ballabio, C., 2020. Plutonium aided reconstruction of caesium atmospheric fallout in European topsoils. *Sci. Rep.* 10, 11858.
- Minato, S., 2002. Simple soil mass balance approach to interpret the distribution of global terrestrial gamma ray dose rates in relation to geology. *Sci. Total Environ.* 298, 229–231.
- Moreno, V., Bach, J., Baixeras, C., Font, L., 2014. Radon levels in groundwaters and natural radioactivity in soils of the volcanic region of La Garrotxa, Spain. *J. Environ. Radioact.* 128, 1–8.
- Navas, A., Walling, D.E., Quine, T., Machín, J., Soto, J., Domenech, S., López-Vicente, M., 2007. Variability in 137Cs inventories and potential climatic and lithological controls in the central Ebro valley, Spain. *J. Radioanal. Nucl. Chem.* 274, 331–339.
- Ngachin, M., Garavaglia, M., Giovani, C., Kwato Njock, M.G., Nourreddine, A., 2008. Radioactivity level and soil radon measurement of a volcanic area in Cameroon. *J. Environ. Radioact.* 99, 1056–1060.
- Pascholati, E.M., Amaral, G., Hiodo, F.Y., Okuno, E., Yoshimura, E.M., Yukihara, E.G., 1997. Survey of environmental gamma radiation around Itu (Sao Paulo State,

- Brazil). In: Proceedings of the 4 Brazilian Meeting on Nuclear Applications v 1, Brazil, p. 646.
- Saleh, E.E., El-Mageed, A.I., El-Kamel, A.H., Abbady, A., Harb, S., 2011. Natural radioactivity in the volcanic field north of Sana'a, Yemen. In: Radiation Protection and Environment, 34.
- Sato, T., 2015. Analytical model for estimating terrestrial cosmic ray fluxes nearly anytime and anywhere in the world: extension of PARMA/EXPACS. PLoS One 10, e0144679.
- Schmincke, H.U., 1982. Volcanic and chemical evolution of the Canary Islands. In: von Rad, U., Hinz, K., Sarnthein, M., Seibold, E. (Eds.), Geology of the Northwest African Continental Margin. Springer.
- Schön, S.J., 2011. Chapter 5 - nuclear/radioactive properties. In: Schön, J.H. (Ed.), Handbook of Petroleum Exploration and Production. Elsevier, pp. 107–148.
- Seaman, J.C., Roberts, K.A., 2012. Radionuclide transport in terrestrial environments. In: Meyers, R.A. (Ed.), Encyclopedia of Sustainability Science and Technology. Springer New York, New York, NY, pp. 8597–8634.
- Shahrokhi, A., Adelikhah, M., Chalupnik, S., Kovács, T., 2021. Multivariate statistical approach on distribution of natural and anthropogenic radionuclides and associated radiation indices along the north-western coastline of Aegean Sea, Greece. Mar. Pollut. Bull. 163, 112009.
- Troll, V.R., Carracedo, J.C., 2016. Chapter 1 - the Canary Islands: an introduction. In: Troll, V.R., Carracedo, J.C. (Eds.), The Geology of the Canary Islands. Elsevier, pp. 1–41.
- Tzortzis, M., Tsertos, H., Christofides, S., Christodoulides, G., 2003. Gamma-ray measurements of naturally occurring radioactive samples from Cyprus characteristic geological rocks. Radiat. Meas. 37, 221–229.
- UNE, 2002a. Procedimiento de toma de muestras para la determinación de la radioactividad ambiental. Parte 1: Suelos, capa superficial. In: Standard 73311–1. Asociación Española de Normalización y Certificación, Madrid.
- UNE, 2002b. Procedimiento para la conservación y preparación de muestras de suelo para la determinación de radioactividad ambiental. In: Standard 73311–5. Asociación Española de Normalización y Certificación, Madrid.
- UNSCEAR, 1982. Report to the General Assembly, with Scientific Annexes. United Nations, New York, pp. 43–82.
- UNSCEAR, 1993. Report to the General Assembly, with Scientific Annexes. United Nations, New York, pp. 33–90.
- UNSCEAR, 2000. Report to the General Assembly, with Scientific Annexes. United Nations, New York, pp. 84–156.
- UNSCEAR, 2008. Report to the General Assembly, with Scientific Annexes. United Nations, New York, pp. 221–463.
- Webb, P.C., 1988. Radioactivity in geology: Principles and applications by E. M. Durrance (Ellis Horwood series in Geology), Ellis Horwood Ltd, Chichester, England, 1986. no. of pages: 441. price: £59.50 (hardback). Geol. J. 23, 104–105.
- Wotawa, G., De Geer, L.-E., Becker, A., D'Amours, R., Jean, M., Servranckx, R., Ungar, K., 2006. Inter- and intra-continental transport of radioactive cesium released by boreal forest fires. Geophys. Res. Lett. 33.